

it is sometimes possible to locate complete breaks among the remaining conformations. There may be boundaries between two adjacent residues which are never included within a single region. This permits treatment of such molecular fragments in a completely independent way.

Application of this reduction to the conformations in Table I shortens the list by eliminating forms 3, 5, 7, 9, 11, 21, 25, 26, 27, 28, 29, 30, 33, 35, 36, and 39. The original 42 forms are reduced to 26 in this way; however, there are no independent fragments since conformation 12, which spans the whole fragment, is retained. If alternation of conformations were not imposed, then the list could be shortened further by retaining only the most favored conformation for each specific region, e.g., by comparing the free energy of  $\alpha_{3-5}$  from Table I with that of  $\beta_{3-5}$  and eliminating  $\alpha_{3-5}$ .

The results obtained by the present method are very similar to those obtained by the authors, using another selection scheme.<sup>2</sup> That "conformation stability" selection can be applied to the set of conformations in Table I. This method follows: (1) all conformations are placed in order by their associated free energies, (2) the most favorable conformation is chosen, (3) the next most favorable form is chosen if it does not include residues previously chosen, and (4) the third step is repeated until every residue is assigned a conformation. Application to the data in Table I yields  $-12.2$  for  $\beta_2\alpha_3\text{--}\alpha_6\alpha_7$  or  $-10.0$  for  $\beta_2\alpha_3\text{--}\beta_6\beta_7$ , depending on whether or not the condition of alternation is imposed. A comparison with the previous examples indicates that there is a tendency for the free energy minimization to yield somewhat shorter, less regular forms than does the conformation stability scheme. The energy minimization scheme would be expected to reflect somewhat more di-

rectly any inadequacies in free energy calculations because it does not depend so much on the effects of averaging over longer segments. Results with both methods are usually approximately the same; this provides an indication that the conformation stability selection gives conformations which closely approximate minimum free energy forms. Both methods yield the most significant feature of the present fragment, namely, the short helix. Experimental X-ray results<sup>7</sup> indicate that the correct form is approximately  $\beta_2\alpha_3\text{--}\beta_6\beta_7\text{--}10$ .

The present energy minimization method yields a global minimum, within the approximation of representing the total free energy as the sum of free energies of independent secondary structure regions. It should be possible to impose inter-region energy calculations at each selection step in the energy minimization method. This might eliminate the problem of choosing too many single independent residue conformations and would incorporate some of the tertiary interactions; however, it may introduce a dependence on the selection pathway.

## References and Notes

- (1) G. Nemethy and H. A. Scheraga, *Q. Rev. Biophys.*, **10**, 239 (1977).
- (2) R. L. Jernigan, S. Miyazawa, and S. C. Szu, to be published.
- (3) R. R. Matheson, Jr., and H. A. Scheraga, *Macromolecules*, **11**, 819 (1978).
- (4) V. I. Lim, *Dokl. Akad. Nauk SSSR*, **222**, 1467 (1975).
- (5) D. T. Phillips, A. Ravindran, and J. J. Solberg, "Operations Research: Principles and Practice", Wiley, New York, 1976, pp 419–468.
- (6) O. B. Ptitsyn and A. V. Finkelstein, *Biophysics*, **15**, 785 (1970).
- (7) R. J. Feldmann, "Atlas of Macromolecular Structure on Microfiche", Structure AM 3.6.1.1.1 Tracor Jitco Inc., Rockville, Md. 1977.

## Infinite-Dilution Oscillatory Flow Birefringence Properties of Four-Armed Star Polystyrene

Alan L. Soli and John L. Schrag\*

Department of Chemistry and Rheology Research Center, University of Wisconsin, Madison, Wisconsin 53706. Received July 27, 1979

**ABSTRACT:** The oscillatory flow birefringence properties (characterized by the magnitude  $S_m$  and relative phase angle  $\theta_s$  of the complex mechanooptic coefficient  $S^*$ ) of solutions containing what were thought to be four-armed polystyrene stars (equal length arms linked with  $\text{SiCl}_4$ ) with narrow distribution number average molecular weights of  $2.34 \times 10^5$  and  $8.58 \times 10^5$  have been measured over a frequency range from  $10^0$  to  $2 \times 10^3$  Hz at several temperatures. The solvent was Aroclor 1248, lot KM 502, a chlorinated biphenyl. The data have been extrapolated to obtain infinite dilution properties which are compared with the predictions of the Zimm–Kilb theory. The fits obtained indicate that the samples have substantial amounts of functionality polydispersity; the supposedly four-arm molecules apparently consist of a mixture of two-, three-, and four-armed structures, with the major component having three arms. Also, the values of the hydrodynamic interaction parameter required to generate theoretical fits to the data are essentially the same as those required to fit infinite dilution oscillatory flow birefringence and viscoelastic properties of linear polystyrenes in Aroclor solvents but are substantially different from those obtained for star polystyrene molecules from infinite dilution viscoelasticity studies. The precision obtainable with the oscillatory flow birefringence technique suggests that it may be a useful method for detecting small amounts of long-chain branching.

There have been several studies of the frequency dependence of the oscillatory flow birefringence (OFB) and viscoelasticity (VE) of linear polymers in solutions sufficiently dilute to enable extrapolation to obtain infinite dilution properties.<sup>1–9</sup> The theory of Zimm<sup>10</sup> has been shown to be in very good agreement at low frequencies with

the above data when exact eigenvalues obtained by the method of Lodge and Wu<sup>11,12</sup> are used. Branched polymers have also been of interest since the long time end of the relaxation spectrum is affected substantially by overall chain topology. Several viscoelastic studies have been reported for polymers with a variety of types of branching, some of which have included extrapolations to obtain infinite dilution properties.<sup>13–19</sup> Again these data have agreed quite well at low frequencies with the Zimm–Kilb theory<sup>20</sup>

\* Address correspondence to this author at the Department of Chemistry.

as evaluated by Osaki and Schrag,<sup>21</sup> although some of the theoretical fits required anomalously high values of the hydrodynamic interaction parameter  $h^*$ .<sup>13,14,18</sup>

This paper describes initial OFB studies of the effect of chain topology on molecular dynamics. Data for two samples thought to be four-armed star polystyrenes have been extrapolated to obtain infinite dilution properties which are compared to predictions of the Zimm-Kilb theory and to earlier VE studies of the identical samples.<sup>13,18,19</sup>

## Experimental Section

**Materials.** The two samples of four-armed star polystyrene were synthesized in the laboratory of Professor S. Onogi of Kyoto University, Japan, via anionic polymerization with *n*-butyllithium catalyst to give living polystyrene arms of narrow molecular weight distribution. These branches were then linked with  $\text{SiCl}_4$  to form the four-armed stars with branches of equal length.<sup>13,18,22</sup> Sample LB-16 has a reported  $M_n$  of  $2.34 \times 10^5$  (osmometry) with a  $M_w/M_n$  ratio of 1.17 (GPC), while the corresponding values for sample LS-13 are  $8.58 \times 10^5$  and 1.29, respectively. These were dissolved in Aroclor 1248, lot KM 502, a chlorinated biphenyl manufactured by the Monsanto Chemical Co. This solvent was selected both for its large dependence of viscosity on temperature and for its close match in index of refraction to polystyrene to minimize form birefringence effects which are not included in the Zimm or Zimm-Kilb theories.<sup>3</sup> Solutions were prepared by weight with moderate heating (40 °C) and very gentle stirring by hand once a day. The highest concentrations were made first, with subsequent dilution to obtain the lower concentrations, primarily due to very limited amounts of sample; this also restricted the number of concentrations studied. The solution concentrations were 0.0188, 0.0117, and 0.00506 g/cm<sup>3</sup> for LB-16 and 0.0165, 0.00933, and 0.00427 g/cm<sup>3</sup> for LS-13 (assuming  $\rho = 1.4523$  and 1.06 g/cm<sup>3</sup> for Aroclor 1248 and the polystyrenes, respectively, and additivity of volumes).

**Method.** The thin fluid layer OFB apparatus used to obtain the measurements has been described previously.<sup>7,8</sup> This system has now been interfaced to a second generation computerized data acquisition and processing system (DAPS) based on a Varian 620/L-101 minicomputer, providing substantial improvement over the lock-in amplifier used in previous studies. The effective frequency range of five decades is double that obtainable with the lock-in, resulting in fewer data runs required to cover a solution's complete relaxation spectrum. In addition, the minimum measurable birefringence (approximately  $10^{-11}$  difference in the principal indices of refraction for  $\pm 1\%$  precision) is two orders of magnitude better than was obtained previously. This enhanced sensitivity is essential for the low concentration studies necessary for reliable extrapolations to obtain infinite dilution properties.

Many of the principles and procedures utilized in the new DAPS are similar to those of the first generation system designed by Massa and Schrag for use with the modified Birnboim and multiple-lumped resonator apparatuses for measurement of solution VE properties.<sup>24-26</sup> Hardware improvements over the old system include faster amplifiers, computer-controlled frequency selection, and more memory.<sup>23</sup> The major change in the data processing is the inclusion of signal averaging which is accomplished in real time during the data acquisition. The combination of this technique for random noise rejection and the previously used cross-correlation methods of the first version of the DAPS<sup>24,25</sup> provides an unexpectedly large enhancement of the noise rejection capability. For example, the measured relative phase angle between two sinusoidally time-varying signals typically will exhibit less than 0.1° of scatter at a signal-to-noise ratio of 1. This level of precision is especially important for these studies since the Aroclor solvent is itself birefringent. Thus, following the procedure of Sadron,<sup>27</sup> it is necessary to subtract off (vectorially) the relatively large (at low concentrations) contribution of the solvent to obtain the net polymer contribution.<sup>3,28</sup>

## Results

The birefringence data obtained at an optical wavelength  $\lambda_0 = 5770 \text{ Å}$  are reported in terms of the frequency de-

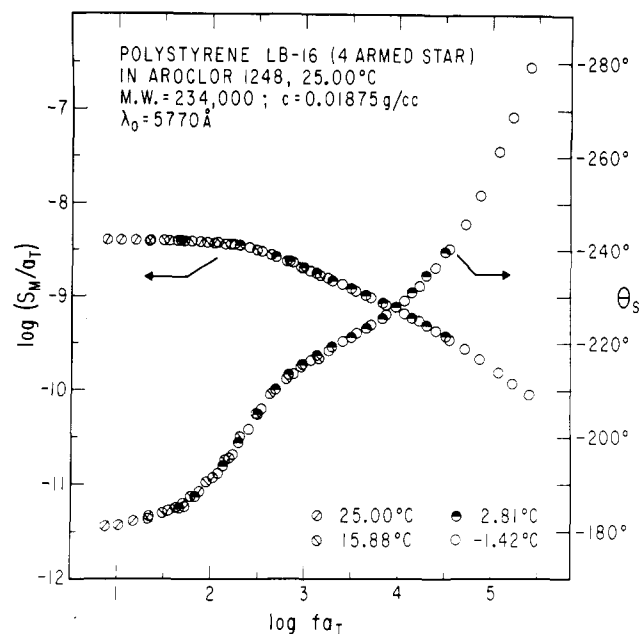


**Figure 1.** Plots of magnitude ( $S_m/a_T$ ) and relative phase angle  $\theta_s$  of the complex mechanooptic coefficient  $S^*$  plotted logarithmically against frequency and reduced to 25.00 °C for the 234 000 molecular weight four-armed star polystyrene/Aroclor solution noted in the figure; data obtained at four temperatures as shown.

pendence of the magnitude  $S_m$  and phase angle  $\theta_s$  of the complex mechanooptic factor  $S^*$  defined as

$$S^* = S_m \exp(i\theta_s) = -\Delta n^* / \dot{\gamma}^* \quad (1)$$

where  $\Delta n$ , the real part of  $\Delta n^*$ , is the difference in indices of refraction  $n_1$  and  $n_2$  in principal directions 1 and 2, and  $\dot{\gamma}$ , the real part of  $\dot{\gamma}^*$ , is the sinusoidally time varying shear rate, as defined previously.<sup>7,8</sup> Measurements were obtained at four temperatures for each solution, and the data were reduced to 25.0 °C reference temperature via time-temperature superposition,<sup>28,29</sup> resulting in reduced variable (logarithmic) plots of  $S_m/a_T$  and  $\theta_s$  vs.  $\log fa_T$  (frequency  $f$  in Hz) as illustrated in Figures 1 and 2 for the highest concentrations of each polymer that were studied. The shift factors  $a_T$  were obtained from the temperature dependence of the low-frequency, frequency-independent  $S_m$  values where possible.<sup>7,8,28</sup> For some low-temperature data, it was necessary to also obtain shift factors from the temperature dependence of the birefringence of the solvent which for Aroclors is essentially identical with the temperature dependence of viscosity.<sup>28</sup> As can be seen from the figures, the superpositions obtained are excellent. Data scatter (before superposition) for  $S_m$  and  $\theta_s$  was under 0.1% and 0.2°, respectively, throughout most of the frequency range for these solutions except for the lowest concentration and/or high frequencies where the solvent birefringence correction becomes large.

For both polymer samples,  $\theta_s$  changed by more than 90° from the steady flow limit, as has been reported earlier for linear polystyrenes.<sup>7,8</sup> The character of the low-frequency data for these branched polymers resembles that of linear polymers as well,<sup>8,30</sup> but there is a marked increase in the sharpness of the knee of the phase curve ( $\log fa_T = 2.5$  to 3 for LB-16 and 1.5 to 2 for LS-13) relative to curves for linear polymers of comparable molecular weights and concentrations.

To obtain infinite dilution properties, values of  $\log (S_m/ca_T)$  and  $\theta_s$  were plotted vs. concentration  $c$ ; sample plots for sample LB-16 are shown in Figure 3 for repre-

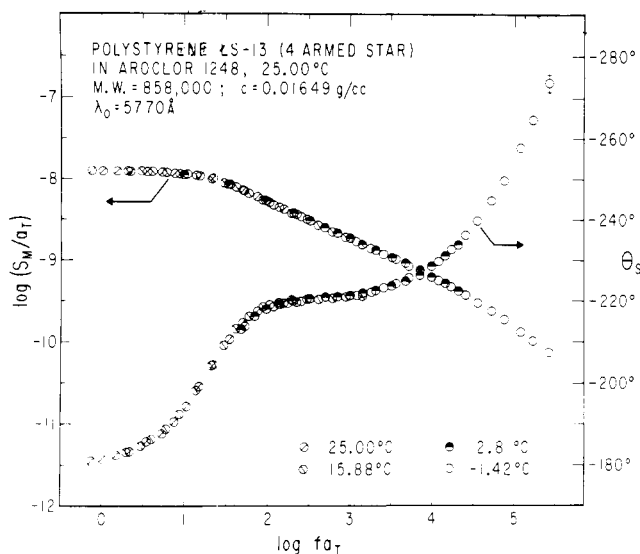


**Figure 2.**  $(S_m/a_T)$  and  $\theta_s$  plotted logarithmically against frequency and reduced to 25.00 °C for the 858 000 molecular weight four-armed star polystyrene/Aroclor solution noted in the figure; data obtained at four temperatures as shown.

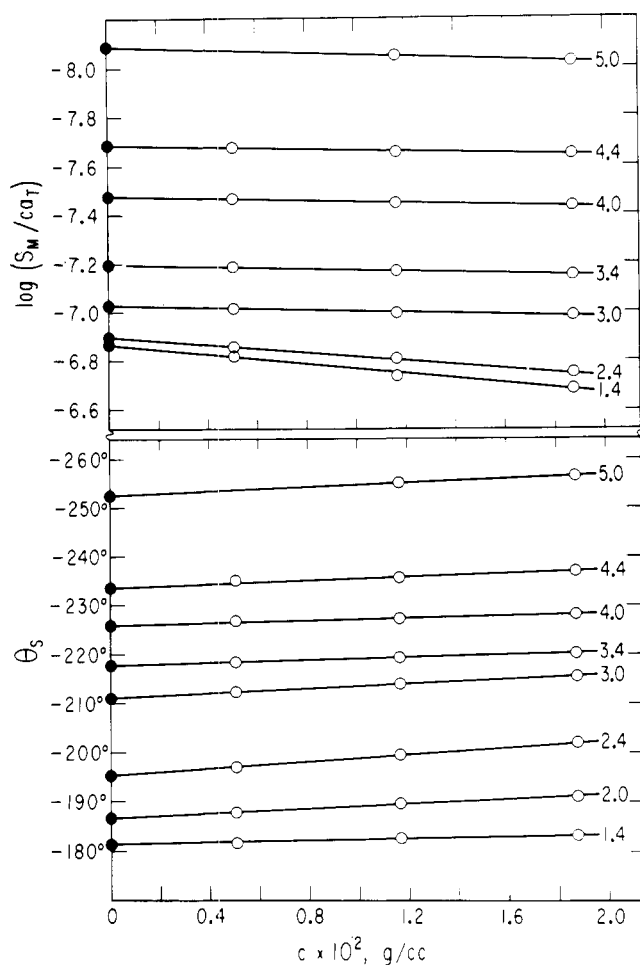


**Figure 3.**  $\log(S_m/ca_T)$  and  $\theta_s$  plotted against concentration for selected values of  $\log(fa_T)$  (shown to the right of each line) to illustrate extrapolation procedures to obtain infinite dilution  $[S_m]$  and  $[\theta_s]$  properties (filled circles); polystyrene LB-16 in Aroclor 1248, data reduced to 25.00 °C.

sentative values of  $fa_T$  (listed at the right end of each line). The extrapolation curves for LS-13 are essentially identical in character. The intercepts of the lines (filled circles) define the intrinsic values  $\log[S_m]$  and  $[\theta_s]$ . Figures 4 and

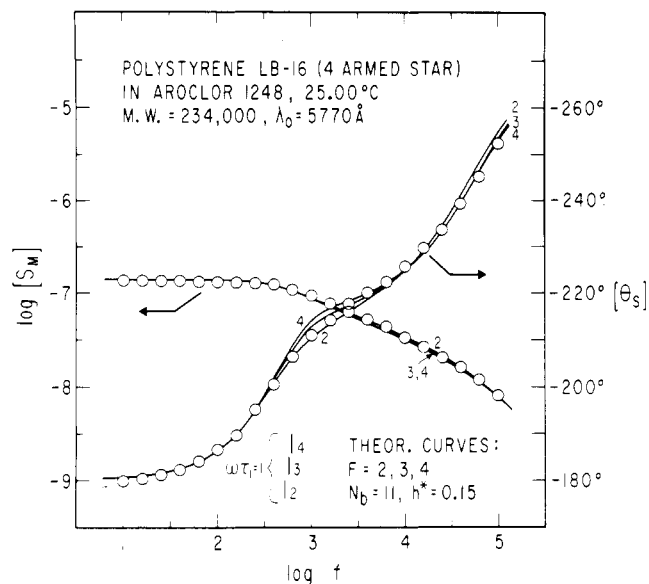


**Figure 4.** Infinite dilution properties  $[S_m]$  and  $[\theta_s]$  plotted logarithmically against frequency at 25.00 °C for the star polystyrene/Aroclor solution noted in the figure; theoretical curves are Zimm-Kilb predictions for  $N_b$ ,  $h^*$ , and  $F$  values listed and are arbitrarily shifted to obtain best fit.  $\log f$  at which each theoretical plot gives  $\omega\tau_1 = 1$  is indicated by short vertical lines subscripted with the appropriate value of  $F$ .

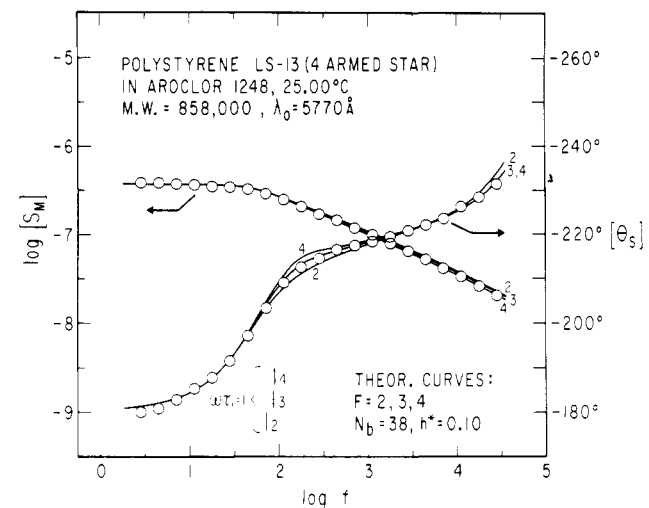


**Figure 5.**  $[S_m]$  and  $[\theta_s]$  plotted logarithmically against frequency at 25.00 °C for the star polystyrene/Aroclor solution noted in the figure; theoretical curves are Zimm-Kilb predictions for  $N_b$ ,  $h^*$ , and  $F$  values listed and are arbitrarily shifted to obtain the best fit.  $\log f$  at which  $\omega\tau_1 = 1$  are indicated by subscripted short vertical lines.

5 present the intrinsic properties for LB-16 and LS-13, respectively. These extrapolations have been carried out in order to examine the topological influence on the observed polymer dynamics, not to study the concentration dependence per se, primarily due to the very limited quantity of sample that was available; this also dictated the use of only three dilutions with the maximum concentrations as noted above. However, extensive studies of concentration dependence of OFB properties of polystyrene/Aroclor solutions have been carried out in these laboratories;<sup>7,9</sup> based on these additional studies and the high degree of reproducibility of the data, the extrapolated properties reported here are expected to have an uncertainty for  $[S_m]$  of less than 3% and for  $[\theta_s]$  of less than 1°. In general, OFB data extrapolations to obtain intrinsic properties of polymer solutions have much less scatter than

comparable VE plots.<sup>1,7,9,25,31</sup>

## Discussion

The curves in Figures 4 and 5 are for the Zimm-Kilb bead-spring model theory<sup>20a,b</sup> incorporating exact eigenvalues calculated by the method of Lodge and Wu,<sup>11,12</sup> assuming star-shaped topology with  $F$  branches of equal length each containing  $N_b$  beads. All branches are linked to a central bead giving  $(N_b F + 1)$  total beads per model molecule. The mechanooptic coefficient defined by eq 1 is given by

$$\frac{S^*}{S_0} = \{(F-1) \sum_{p_{\text{odd}}=1}^{2N_b-1} [(\lambda_1/\lambda_p)[1 - i\omega\tau_1(\lambda_1/\lambda_p)]\} / \{1 + (\omega\tau_1)^2(\lambda_1/\lambda_p)^2\} + \sum_{p_{\text{even}}=2}^{2N_b} [(\lambda_1/\lambda_p)[1 - i\omega\tau_1(\lambda_1/\lambda_p)]\} / \{1 + (\omega\tau_1)^2(\lambda_1/\lambda_p)^2\}\} / \{(F-1) \sum_{p_{\text{odd}}=1}^{2N_b-1} \lambda_1/\lambda_p + \sum_{p_{\text{even}}=2}^{2N_b} \lambda_1/\lambda_p\} \quad (2)$$

where  $S_0$  is the steady flow limit of  $S^*$ ,  $\lambda_p$  is the  $p$ th eigenvalue of the Zimm  $\mathbf{H} \cdot \mathbf{A}$  matrix,<sup>20</sup>  $\omega$  is the angular frequency,  $\tau_1$  is the longest relaxation time, and  $i = -1^{1/2}$ . The primary effect of the star geometry is to weight the odd- and even-numbered modes differently. Curves are shown for functionality  $F = 2, 3$ , and 4, since it has been reported that when chlorosilanes are used to link polystyrene segments to form star structures, steric factors which can lead to substantial bond strains result in less than complete linking.<sup>32-34</sup> Thus it is probable that both the LB-16 and LS-13 samples contain appreciable amounts of two- and three-armed stars in addition to the desired four-armed structure. In synthesis, the linear branches (with very narrow molecular weight distribution) are linked to form the stars; thus  $N_b$  is kept constant for each theoretical curve for a given sample. The curves were empirically positioned to obtain the best fits to the data in the  $\omega\tau_1 = 1$  region (the model-dependent values of  $\omega\tau_1 = 1$  for each value of  $F$  are indicated by short vertical lines below the curves). Sample quantities precluded  $[\eta]$  determinations for absolute positioning of the theoretical curves.<sup>1,29</sup> The values of the hydrodynamic interaction parameter shown in Figures 4 and 5 were those that provided optimum fits in the frequency regime around  $\omega\tau_1 = 1$  and are in good agreement with values obtained from OFB and VE studies of linear polystyrenes.<sup>1,2,7-9</sup> For both samples, the curves for  $F = 3$  provide the best fit but clearly differ from the data, indicating that the samples contain mixtures of significant amounts of two-, three-, and four-armed stars, with the major fraction being three-armed structures.

Viscoelasticity measurements have previously been carried out and extrapolated to infinite dilution for both LB-16 and LS-13, using the multiple-lumped resonator.<sup>9,10</sup> A surprising result of these studies was the unusually large value of  $h^*$  required to generate theoretical curves that fit the data. In a  $\Theta$  solvent, values of  $h^* = 0.40$  were required, whereas  $\Theta$  conditions are expected to correspond to  $h^* \approx 0.22$ <sup>11,12</sup> as has been found for linear polystyrenes.<sup>1,29</sup> Similar large values of  $h^*$  were necessary to fit data for a nine-armed star polystyrene;<sup>14</sup> the data were fit with  $h^* = 0.40$  in two different  $\Theta$  solvents and 0.25 for a good solvent. The VE properties of LS-13 have also been measured at finite concentrations in an Aroclor solvent with the modified Birnboim apparatus;<sup>19</sup> an  $h^* = 0.09$  was required to fit the data obtained at the lowest measured concentration (0.0181 g/mL). The VE data obtained at finite concentrations for LS-13 are in reasonable agreement with the OFB results reported here. It is expected that  $h^*$  will increase as  $\Theta$  conditions are approached, but the physical significance of a value exceeding  $h^* = 0.22$  is

unclear. Since VE properties are substantially more difficult to obtain than OFB, the scatter seen in such plots tends to mask what may be small deviations from theory. Thus the previous VE results were compared with theoretical curves calculated assuming no functionality polydispersity; it may be that the large values of  $h^*$  required to obtain fits are in part a result of this assumption.

In summary, some previous VE data have indicated that branching enhances hydrodynamic interaction.<sup>13,14,18</sup> However, contradictory VE evidence exists for polybutadienes in a good solvent where  $h^* = 0.1$  was required for a four-armed star while  $h^* = 0.15$  was necessary for a linear molecule.<sup>3</sup> In view of the apparent functionality polydispersity of both the LS-13 and LB-16 samples, it is difficult to establish the influence of polymer branching on the theoretical hydrodynamic interaction parameter required to obtain curve fits for either the OFB or VE data. In fact, because of this polydispersity problem, previous VE data for polystyrene stars referenced herein—as well as the present OFB study—probably are not quantitatively stringent tests of theory or of the utility of these methods for determining molecular topology. However, the qualitative aspects of the observed topological influences on OFB and VE properties—such as the bump appearing in the  $(G'' - \omega\eta_s)$  and  $\theta_s$  curves in the  $\omega\tau_1 = 1$  frequency regime, the decrease in  $G'$  relative to  $(G'' - \omega\eta_s)$  for  $\omega\tau_1 < 1$ , and the shift of  $\omega\tau_1 = 1$  with functionality shown in Figures 4 and 5—are correct. The high precision obtainable with the OFB technique suggests that it may be a useful method for exploring molecular topology and for detecting small amounts of long-chain branching for appropriately monodisperse samples.

Future OFB and VE studies are being planned on homopolymer star molecules with various functionalities and low functionality polydispersity in a variety of different solvents to reexamine the effect of branching on chain dynamics.

**Acknowledgment.** This work was supported by the National Science Foundation through Grant No. DMR76-81715. We wish to express our appreciation to Professor J. D. Ferry for many helpful discussions of this work.

## References and Notes

- (1) R. M. Johnson, J. L. Schrag, and J. D. Ferry, *Polym. J.*, **1**, 742 (1970).
- (2) K. Osaki, J. L. Schrag, and J. D. Ferry, *Macromolecules*, **5**, 144 (1972).
- (3) K. Osaki, Y. Mitsuda, R. M. Johnson, J. L. Schrag, and J. D. Ferry, *Macromolecules*, **5**, 17 (1972).
- (4) T. C. Warren, J. L. Schrag, and J. D. Ferry, *Macromolecules*, **6**, 467 (1973).
- (5) R. W. Rosser, N. Nemoto, J. L. Schrag, and J. D. Ferry, *J. Polym. Sci., Polym. Phys. Ed.*, **16**, 1031 (1978).
- (6) R. W. Rosser, J. L. Schrag, and J. D. Ferry, *Macromolecules*, **11**, 1060 (1978).
- (7) J. W. Miller, Ph.D. Thesis, University of Wisconsin, Madison, WI, 1979.
- (8) J. W. Miller and J. L. Schrag, *Macromolecules*, **8**, 361 (1975).
- (9) T. P. Lodge, J. W. Miller, and J. L. Schrag, in preparation.
- (10) B. H. Zimm, *J. Chem. Phys.*, **24**, 269 (1956).
- (11) A. S. Lodge and Y. Wu, University of Wisconsin Rheology Research Center Report No. 16, Madison, WI, 1972.
- (12) A. S. Lodge and Y. Wu, *Rheol. Acta*, **10**, 539 (1971).
- (13) Y. Mitsuda, Ph.D. Thesis, University of Wisconsin, Madison, WI, 1973.
- (14) Y. Mitsuda, K. Osaki, J. L. Schrag, and J. D. Ferry, *Polym. J.*, **4**, 24 (1973).
- (15) Y. Mitsuda, J. L. Schrag, and J. D. Ferry, *Polym. J.*, **4**, 668 (1973).
- (16) Y. Mitsuda, J. L. Schrag, and J. D. Ferry, *J. Appl. Polym. Sci.*, **18**, 193 (1974).
- (17) N. Nemoto, Y. Mitsuda, J. L. Schrag, and J. D. Ferry, *Macromolecules*, **7**, 253 (1974).

- (18) Y. Mitsuda and J. D. Ferry, *Kobunshi Ronbunshu*, **31**, 135 (1974).
- (19) J. W. M. Noordermeer, O. Kramer, F. H. M. Nestler, J. L. Schrag, and J. D. Ferry, *Macromolecules*, **8**, 539 (1975).
- (20) (a) B. H. Zimm and R. W. Kilb, *J. Polym. Sci.*, **37**, 19 (1959);  
(b) K. Osaki, Y. Mitsuda, J. L. Schrag, and J. D. Ferry, *Trans. Soc. Rheol.*, **18**, 395 (1974).
- (21) K. Osaki and J. L. Schrag, *J. Polym. Sci., Polym. Phys. Ed.*, **11**, 549 (1973).
- (22) T. Masuda, Y. Ohta, and S. Onogi, *Macromolecules*, **4**, 763 (1971).
- (23) A. L. Soli, Ph.D. Thesis, University of Wisconsin, Madison, WI, 1978.
- (24) D. J. Massa, Ph.D. Thesis, University of Wisconsin, Madison, WI, 1970.
- (25) D. J. Massa and J. L. Schrag, *J. Polym. Sci., Part A-2*, **10**, 71 (1972).
- (26) M. H. Birnboim, J. S. Burke, and R. L. Anderson, "Proceedings of the Fifth International Congress on Rheology", Kyoto, S. Onogi, Ed., University Park Press, Baltimore, MD, 1969, p 409.
- (27) C. Sadron, *J. Phys. Radium*, **9**, 381 (1938).
- (28) J. L. Schrag, Ph.D. Thesis, Oklahoma State University, Stillwater, OK, 1967.
- (29) J. D. Ferry, "Viscoelastic Properties of Polymers", 2nd ed., Wiley, New York, 1970.
- (30) G. B. Thurston and J. L. Schrag, *J. Polym. Sci., Part A-2*, **6**, 1331 (1968).
- (31) J. L. Schrag and J. D. Ferry, *Faraday Symp. Chem. Soc.*, **No. 6**, 182 (1972).
- (32) N. Hadjichristidis, A. Guyot, and L. J. Fetters, *Macromolecules*, **11**, 668 (1978).
- (33) J. E. L. Roovers and S. Bywater, *Macromolecules*, **5**, 385 (1972).
- (34) M. Nagasawa, private communication.

## Estimation of Solubility Parameters for Some Olefin Polymers and Copolymers by Inverse Gas Chromatography

K. Ito<sup>1</sup> and J. E. Guillet\*

*Department of Chemistry, University of Toronto, Toronto, Canada M5S 1A1.  
Received May 22, 1979*

**ABSTRACT:** Flory–Huggins  $\chi$  parameters have been determined by gas chromatography at 30 °C for ten standard hydrocarbons in ethylene (40%)–propylene (60%) copolymer, *cis*-polyisoprene, and amorphous polypropylene to estimate the polymer solubility parameter ( $\delta_2^\infty$ ) by the method developed by DiPaola-Baranyi and Guillet. The results are as follows:  $\delta_2^\infty = 7.70 \pm 0.11$  for ethylene–propylene,  $7.96 \pm 0.10$  for *cis*-polyisoprene, and  $7.67 \pm 0.16$  for polypropylene. The parameters for ethylene–propylene were also estimated by extrapolation from the higher temperature data (63–83 °C) and found to be in good agreement with those estimated directly.

The solubility parameter concept has been used extensively in practical applications of polymers. DiPaola-Baranyi and Guillet<sup>2</sup> have recently shown that inverse gas chromatography, using a polymer as the stationary phase, can be a simple and convenient method for estimating solubility parameters for polymers. The method is based on the principle that the Flory–Huggins  $\chi$  parameter can be readily determined from retention data on various small molecule probes and that  $\chi$  can be related to solubility parameters by Hildebrand–Scatchard theory<sup>4</sup> combined with Flory theory,<sup>5</sup> as follows:

$$\chi = (V_1/RT)(\delta_1 - \delta_2)^2 \quad (1)$$

where  $\chi$  has free-energy characteristics, i.e.,

$$\chi = \chi_H + \chi_S \quad (2)$$

and  $V_1$  is the molar volume of the probe used,  $\delta_1$  is the solubility parameter of the probe, and  $\delta_2$  is the solubility parameter of the polymer. In the usual experiment,  $\chi$  is determined under conditions approximating infinite dilution of the probe in the polymer, and hence the value of  $\delta_2$  is more correctly designated  $\delta_2^\infty$ , since it is also an infinite dilution quantity. For reasons outlined previously,<sup>2</sup> this quantity may have more fundamental significance than the value of  $\delta_2$  measured at finite solute concentrations by classical methods such as swelling or solubility measurements. Furthermore, at the high dilution of the experiment, it is possible that the assumptions of regular solution behavior, inherent in the Hildebrand–Scatchard treatment, are more closely fulfilled.

The method has been successfully applied to estimate consistent  $\delta_2^\infty$  values for polystyrene at 193 °C, poly(methyl

acrylate) at 100 °C, and poly(vinyl acetate) at 135 °C, using a variety of standard hydrocarbon solutes of different  $\delta_1$  values.  $\delta_2^\infty$  was also estimated at 25 °C, using  $\chi$  parameters computed by extrapolation of the higher temperature data according to

$$\chi = \alpha + \beta/T \quad (3)$$

where the constants  $\alpha$  and  $\beta$  should have characteristics of entropy and enthalpy, respectively. This empirical equation is usually valid only for relatively small ranges of temperature; however, the  $\delta_2^\infty$  values thus obtained were shown to agree well with literature data, supporting the idea that the derived parameters might be practically useful in predicting polymer solubility even at finite concentrations.

The present work extends the method to polymers including ethylene–propylene copolymer (EPR), *cis*-polyisoprene (PIP), and amorphous polypropylene (PP). Since these polymers have very low glass-transition temperatures (–20 °C or lower), the GLC data can be obtained close to room temperature, so that their  $\delta_2^\infty$  values can be determined directly and compared with those estimated by the extrapolation method. It will also be shown that the  $\chi$  parameters are more properly expressed by the relation derived by Huggins<sup>7</sup> and by Scott and Magat:<sup>8</sup>

$$\chi = (V_1/RT)(\delta_1 - \delta_2)^2 + \gamma \quad (4)$$

where  $\gamma$  is an entropy correction term which is often considered to be a constant near 0.3 for many polymers.<sup>8,9</sup>

### Experimental Section

Ethylene–propylene rubber was Exxon Vistalon 404 with a composition of 40% ethylene and 60% propylene. *cis*-Poly-